bioRxiv preprint doi: https://doi.org/10.1101/510362; this version posted January 3, 2019. The copyright holder for this preprint (which was not certified by peer review) is the author/funder. All rights reserved. No reuse allowed without permission.

Polar-like trophoblast stem cells form an embryonic-abembryonic axis in blastoids.

Authors:
Javier Frias-Aldeguer[1,2],Maarten Kip[2], Judith Vivié[2], Linfeng Li[1], Anna Alemany[2], Jeroen Korving[2], Frank Darmis[2], Clemens A. Van Blitterswijk[1], Alexander van Oudenaarden[2], Niels Geijsen[2], Nicolas C. Rivron[1,2]

1. Merln Institute for technology-driven regenerative medicine, Maastricht University, The Netherlands
2. Hubrecht Institute for developmental biology and stem cell research, Utrecht, The Netherlands.

Correspondence should be addressed to:
Nicolas Rivron nicolasrivron@gmail.com

Abstract:

Early mammalian embryos form a blastocyst, a structure comprising embryonic cells surrounded by a trophoblast cyst able to implant into the mother's uterus. Following subtle symmetry-breaking events (Zhang and Hiiragi, 2018)**, an axis forms in the blastocyst when the embryonic cells cluster on one inner side of the trophoblast globe and induce the directional proliferation and differentiation of trophoblasts** (Gardner, 2000)**. Trophoblast stem cells (TSCs) are in vitro analogs of early trophoblasts** (Tanaka et al., 1998)**. Here, we show that TSCs contain a range of plastic subpopulations reflecting aspects of trophoblasts states ranging from the blastocyst trophoblasts juxtaposing the embryo (polar trophoblasts) to post-implantation trophoblasts. However, when exposed to a specific combination of embryonic inductive signals, TSCs acquire properties of polar trophoblasts (gene expression, self-renewal) and a more homogeneous, epithelial phenotype. These lines of polar-like TSCs more efficiently form blastoids, which respond to the inner embryonic cells by spontaneously generating an embryonic-abembryonic axis. Altogether, the delineation of requirements and properties of the polar cells of the trophectoderm provides the ground to better recapitulate and dissect embryonic development in vitro.**

Results:

The transcriptome of polar and mural trophoblasts.

In the blastocyst, trophoblasts transition from a proliferative "polar" state juxtaposing the inner cell mass and with stem cell properties, to a more differentiated "mural" state opposite (Gardner, 2000). Indeed, we observed that, as blastocysts progress, Cdx2 expression decreases in the mural trophoblasts (Cdx2 mRNA in E4.5 blastocyst Fig. 1A and Cdx2 immunofluorescence of E3,5 blastocyst cultured for 6 hours, Fig. 1B and Sup. Fig. 1A). Similarly, TSCs cultured in vitro display intercellular heterogeneity for Cdx2 (Fig 1C, Cdx2-eGFP TSCs (McDole and Zheng, 2012)) as also noted previously (Kuales et al., 2015; Motomura et al., 2016).

We analyzed the intercellular heterogeneity of the trophectoderm using an already available dataset of single cells harvested from the polar or mural sites of E4.5 blastocysts (Nakamura et al., 2015). We confirmed that the transcriptomes of polar and mural cells are different (unsupervised gene expression

bioRxiv preprint doi: https://doi.org/10.1101/510362; this version posted January 3, 2019. The copyright holder for this preprint (which was not certified by peer review) is the author/funder. All rights reserved. No reuse allowed without permission.

clustering, Fig. 1D). 1585 genes were differentially expressed (FC>1.5, p-value< 0.001, Sup. Fig. 1B, Sup. table 1) including Cdx2, Esrrb, Ddah1 and Ly6a (Fig. 1E, list of genes in Sup table 1). We also analysed the transcriptome of CDX2-High and CDX2-Low TSCs (1000 cells sorted from top and bottom 5% CDX2-eGFP expressing cells, 1G). 1941 genes were differentially expressed (fc>1.5, p-value<0.01, Sup. table 2). Gene ontology showed that CDX2-High TSCs were enriched for cell cycle, Hippo and Notch pathways, which regulate trophectoderm development (Menchero et al., 2017) (DAVID GO, Sup Fig. 1C, Sup. table 3). CDX2-High population also contained more abundant polar transcripts Cdx2, Esrrb, Ddah1 and Ly6a, while the CDX2-Low population showed higher expression of the mural markers Krt8, Gata2, Slc2a3 (Nakamura et al., 2015; Rivron et al., 2018b). We concluded that CDX2-High TSCs feature aspects of polar trophoblasts.

Trophoblast stem cells contain multiple subpopulations reflecting blastocyst and post-implantation stages.

To delineate the heterogeneity of TSCs, we performed single cell transcriptomic (330 TSCs and 332 differentiated TSCs cultured for 6 days without growth factors). Unsupervised gene clustering analysis separated both cultures and their subpopulations (Fig. 1F). Among the TSCs, fifty percent formed 3 clusters that show higher expression of polar genes Cdx2, Eomes and Esrrb, while another subpopulation expressed Ascl2 concomitant with lower levels of Cdx2 and Eomes, suggestive of an ExE phenotype (Guillemot et al., 1994). Finally, a subpopulation of TSCs (10%) expressed Gcm1, Gjb2 and Flt1, and overlapped with the transcriptome of differentiated trophoblasts suggesting that TSCs include differentiated cells (Fig. 1F).

Single TSCs arranged along a pseudotime trajectory (Sup. Fig. 1D) (Trapnell et al., 2014) with low pseudotime values corresponding to TSCs expressing higher levels of Cdx2, Esrrb, Eomes, Elf5 (Sup Fig. 1F) and high pseudotime values corresponding to differentiated cells expressing Flt1 (spongiotrophoblast (Hirashima et al., 2003)) or Gcm1 (syncytiotrophoblast trophoblasts). The TSC sub-population expressing the post-implantation extra-embryonic ectoderm gene Ascl2 (Guillemot et al., 1994) had intermediate values (Sup. Fig. 1F). Consistent with our previous analysis, some TSCs also had the high pseudotime values of differentiated cells (4.2%, Sup Fig. 1D). We extracted the main genes defining such trajectory (Sup. Fig. 1 G).

Single molecule FISH against Cdx2 and Ascl2 mRNAs in TSCs confirmed that some cells concomitantly expressed high levels of Ascl2 transcripts and low levels of Cdx2 mRNA (Fig. 1H). These cells were mainly located in the central part of colonies. In contrast, cells on the edges are more abundant in Cdx2 transcripts. Finally, some TSCs more highly expressed the genes Krt8 and Krt18, which clearly anti-correlated with Cdx2 immunofluorescence (Krt8/18 immunofluorescence, Fig. 1I).

All together, we concluded that TSCs contain multiple populations ranging from Cdx2/Eomes/Esrrb-High cells reminiscent of the polar trophectoderm to Ascl2-High cells and Krt8/18-High cells (5-10%) reflecting post-implantation trophoblasts.

The Cdx2-high cells have the proliferative and self-renewing features of polar trophoblasts.

We then challenged TSCs in functional assays. First, we sorted CDX2-High and CDX2-Low TSCs and cultured them separately. Within 3-5 days, cells re-established their initial heterogeneity (Sup. Fig. 1H). We concluded that intercellular heterogeneity is an intrinsic property maintaining an equilibrium of sub-populations under these culture conditions. Cell cycle analysis showed that the CDX2-High cells were present in all phases of the cell cycle, while the CDX2-Low cells were predominantly in the G1 phase (Fig. 1J), thus not going through the whole cell cycle. Finally, we tested the potential for self-renewal by examining the clonogenicity of isolated TSCs. Single CDX2-High cells formed 3 times more colonies as compared to CDX2-Low cells (Fig. 1K). Consistent with stem cell properties and with previous experiments showing that the polar trophoblasts are more proliferative and sustain the development of the placenta (Gardner, 2000), our data show CDX2-High TSCs have an an enhanced potential for proliferation and self-renewal.

Altogether, we concluded that TSCs contain heterogeneous subpopulations including CDX2-High cells with features of polar trophoblasts (proliferation, self-renewal, enhanced expression of Cdx2, Esrrb, Ddah1 and Ly6a) and CDX2-Low cells reflecting aspects of mural and post-implantation trophoblasts such as a higher expression of Ascl2 and Krt18 together with lower potential for proliferation and self-renewal. These states are plastic and convertible. These observations are

bioRxiv preprint doi: https://doi.org/10.1101/510362; this version posted January 3, 2019. The copyright holder for this preprint (which was not certified by peer review) is the author/funder. All rights reserved. No reuse allowed without permission.

consistent with the fact that TSCs can be derived from all stages between E3.5 and E8.5 (Tanaka et al., 1998), and suggests the existence of an unaltered and/or reversible pool of trophoblast stem cells.

Combined embryonic inductive signals generate CDX2-High trophoblast stem cells.

We and others have previously showed that inductive signals originating from the inner embryonic cells are necessary to sustain trophoblast proliferation and self-renewal (Gardner, 2000; Rivron et al., 2018b; Tanaka et al., 1998). Here, we reasoned that a combination of embryonic inductive signals could modulate the heterogeneity of TSCs and enrich in the polar-like state. We thus formed a library of compounds (Sup. Table 4) based on the pathways active in the trophectoderm (Sup. Fig. 2A) and on ligands present in the blastocyst (Sup. Fig. 2B). We initially tested these compounds individually for Cdx2-eGFP expression in chemically-defined Tx culture conditions on Matrigel-coated plates, Fig. 2A Sup. Fig. 2C (Kubaczka et al., 2014)). We found 9 compounds (Il11, 8Br-cAMP, Activin, XAV939, Bmp4, Bmp7, LPA, Retinoic Acid and Rosiglitazone) regulating Cdx2 expression in a dose-dependent fashion (Sup. Fig. 2D, >125% Cdx2-high cells, Cdx2-High/Cdx2-Low ratio*100). Because these signals are likely to act synergistically, we used factorial design to explore the combinatorial landscape and compounds interactions (Hutchens et al., 2007). We cultured Cdx2-eGFP TSCs for 10 passages in 21 different cocktails (Fig. 2B left, using each compound's optimal concentration, half that concentration or absent) while monitoring CDX2 expression at each passage (Fig. 2B right). All cocktails lead to initial upregulation of CDX2 expression; however, most cultures (17/21) collapsed after two passages due to a lack of proliferation or attachment. These combinations are likely to induce trophoblast post-mitotic differentiation. Four conditions led to a sustainable, long-term increase in CDX2 expression. Principal component analysis identified Il11, 8-Br cAMP, BMP7 and LPA as beneficial for CDX2 expression while XAV939, Rosiglitazone and Retinoic Acid were detrimental (data from single compounds and combinations, Sup. Fig. 2E-F).

TSCs cultured in these four conditions (10 passages) expressed Cdx2, Eomes, Esrrb, Elf5 and did not markedly upregulate markers of trophoblast differentiation (Sup. Fig. 2G). We selected one condition (Tx21) based on the high expression of Cdx2, Eomes (trophectoderm markers) and on the downregulation of the ExE marker Ascl2 (Sup. Fig. 2H). This culture medium contains Fgf4 (25 ng/ml), Tgfb1 (2 ng/ml), activin (50 ng/ml), Il11 (50 ng/ml), BMP7 (25ng/ml), cAMP (200 nM) and LPA (5nM).

Chemically-defined culture conditions for trophoblast stem cells.

To obtain fully chemically-defined culture conditions, we then tested specific laminin proteins to replace Matrigel coatings (Sup. Fig. 2I). Three laminins (L221, L511 and L521) permitted the culture TSCs without decreasing proliferation or Cdx2 expression. We selected laminin 521 based on the expression of Lamb2 in the blastocyst (Sup. Fig. 2J). The combination of Tx21 medium and laminin 521 coating further increased CDX2 expression and depleted the CDX2-Low sub-population (Fig. 2C and Sup. Fig. 2K). We termed this new culture condition LT21. Of note, TSCs grown in LT21 culture conditions displayed a cobblestone-like phenotype often observed in epithelial cell types and consistent with the trophectoderm of the blastocyst (Fig. 2D).

We derived new lines of TSCs in Tx21 conditions. Due to a lack of initial attachment and proliferation of blastocysts on Laminin 521, the first two passages made use of a layer of mouse embryonic fibroblasts (mEFs, Sup. Fig. 2L). After 3-4 days, the outgrowths expressed trophoblast markers CDX2 and EOMES and showed a decreased degree of differentiation as compared to Tx culture conditions (reduction of CDX2/EOMES negative cells, Fig. 3D). Upon further culture, new cell lines were established (pTS1, Sup. Fig. 2M).

The transcriptome of LT21 TSCs resembles the transcriptome of polar trophoblasts.

Overall, LT21 TSCs are transcriptionally different from TSCs (Sup. Fig. 3A, B, Sup. table 6), increase the expression of the transcription factor circuitry (Cdx2, Esrrb, Eomes), of signaling pathways regulators (Il11, Actvr1, Furin), and of polar genes such as Ly6a and Gsto1.

Single LT21 TSCs have lower pseudotime values as compared to TSCs and differentiated TSCs (6 days without growth factors, Fig. 2F). Consistent with the heterogeneity of TSCs, a subpopulation of these cells are transcriptionally similar to LT21 TSCs, while another one is similar to differentiated TSCs (Fig 2G and Sup. Fig. 3E). Based on gene expression, we propose that the subpopulation of

bioRxiv preprint doi: https://doi.org/10.1101/510362; this version posted January 3, 2019. The copyright holder for this preprint (which was not certified by peer review) is the author/funder. All rights reserved. No reuse allowed without permission.

TSCs similar to the LT21 TSCs represent the polar-like TSCs. We extracted in an unbiased way the top genes defining the pseudotime trajectory (Sup. Fig. 3D). Amongst the 50 genes that describe the low pseudotime were Duox2 and Gsto1, which were previously described as markers for bona fide TSCs (Kuales et al., 2015) and polar trophectoderm (Nakamura et al., 2015). Differentiation markers including Cited2, Gjb2 and Nrk (Imakawa et al., 2016; Morioka et al., 2017; Sood et al., 2006a) had higher pseudotime values.

LT21 TSCs have enhanced self-renewal and chimerize the placenta.

Functionally, LT21 TSCs have cell cycle profiles similar to TSCs (Fig. 3F) but have an enhanced potential for clonogenicity when plated as single cells (2,2-fold, Fig. 3G). This reflects an enhanced ability for growth and viability. Upon growth factor removal, LT21 TSCs rapidly differentiate by decreasing the expression of the trophectoderm markers Cdx2 (day 1) and expressing the ExE markers Ascl2 (peak after three days, Fig. 3H) (Latos et al., 2015). This suggests that LT21 TSCs reflect a preimplantation stage that rapidly passes through a post-implantation stage upon differentiation. Upon six days of differentiation from control and LT21 culture conditions, 3609 and 4190 genes were differentially expressed respectively, among which 3071 genes were common. We concluded that the initial culture conditions do not alter the differentiation potential. Accordingly, upon injection into a blastocyst, both the converted or newly-derived LT21 TSCs contributed to placenta formation (Fig. 3E left and right, respectively, also Sup. Fig. 2N). These results show that LT21 TSCs have an enhanced potential to self-renew, while maintaining their potential to rapidly differentiate.

LT21 TSCs have enhanced epithelial features.

LT21 TSCs were enriched in transcripts related to epithelial development including extracellular matrix organization, cell adhesion, pathways related to ECM-receptor interaction, focal adhesion, cytoskeleton and tight junctions (Sup. table 7). Especially, genes encoding for the adherence molecule Epcam and the tight junction molecules Cldn4, Cldn6, Tjp2, and Jam2 were upregulated (Sup. Fig. 3C). Of note, Cldn4 and Cldn6 have been shown to be essential for blastocyst formation (Moriwaki et al., 2007). We further investigated these changes by measuring the morphometric characteristics of single cells. E-Cadherin and Hoechst segmented the plasma membrane and nucleus respectively, which, along with CDX2 immunofluorescence (Fig. 3A), permitted to automatically extracted 161 morphometric features from both TSCs (502 cells) and LT21 TSCs (297 cells). We ranked these features based on the p-value scores (Mann-Whitney, sup. table 5) and the top 20% morphometric features clearly separated the two cell populations (Fig. 3B). Overall, LT21 TSCs have a larger cell and nuclei area, are more circular and less lobulated (Fig. 3C). Finally, we measured that the morphometric heterogeneity of LT21 TSCs was reduced as compared to TSCs (average distance of each cell to the population centroid for 100 tSNE maps, Sup. Fig. 3F bottom). We concluded that LT21 TSCs are morphologically more homogeneous and with enhanced epithelial morphometric features and gene expression profile (Epcam, Cldn4/6, Jam2, Tjp2), consistent with a preimplantation phenotype.

Altogether, we concluded that these novel culture conditions maintain TSCs in a more homogeneous and epithelial state with a higher self-renewing potential and a gene expression pattern consistent with the polar trophectoderm.

Embryonic inductions contribute to forming blastoids with an embryonic-abembryonic axis.

Blastoid are stem cell-based models of the blastocyst recapitulating aspects of trophectoderm development (Rivron, 2018; Rivron et al., 2018a, 2018b). Here, we reasoned that the presence of subpopulations resembling post-implantation trophoblasts might limit the capacity of TSCs to form a trophectoderm-like structure. Accordingly, LT21 TSCs lines formed blastoids more efficiently as compared to TSCs (Fig. 4A). Blastoids generated from LT21 TSCs correctly localized the basal adherens junctions (E-cadherin) and apical cytoskeletal protein (Krt8/18) typical of an epithelium (Fig. 4D-E). Importantly, blastoids obtained from plTSCs allow for formation of primitive endoderm (Sup. Fig 4G).

bioRxiv preprint doi: https://doi.org/10.1101/510362; this version posted January 3, 2019. The copyright holder for this preprint (which was not certified by peer review) is the author/funder. All rights reserved. No reuse allowed without permission.

Because embryonic inductions are crucial to trophectoderm development (Gardner, 2000; Rivron et al., 2018b), we compared the morphological features of blastoids (comprising inductive ESCs) and trophospheres (formed only with TSCs). Blastoids formed with LT21 TSCs were larger, more circular, and more efficient at forming a cavity as compared to TSCs (Fig. 4B-C and Sup. Fig. 4B and 4D-E). However, only circularity and cavitation efficiency were improved in trophospheres formed with LT21 TSCs (Sup. Fig. 4D-E). Because LT21 TSCs did not proliferate more as compared to TSCs (Sup. Fig. 4C), we concluded that these cells had an enhanced potential to form a cystic cavity, and responded to the embryonic signals by enhancing the cyst diameter.

We then wondered if the embryonic inductions would pattern the trophectoderm-like cyst thus recapitulating aspects of the embryonic-abembryonic axis. Upon single cell isolation from blastoids and further sequencing (Sup. Fig. 4H), the trophoblasts of blastoids formed a pseudotime trajectory (Fig. 4F) including three subpopulations, one of them being a transition between the two others (Fig. 4G). The subpopulation with low pseudotime values expressed higher Cdx2, Eomes, Sox2, Esrrb and the cell cycling marker Ki67 (Sup. table 8 and Fig. 4H-I) along with numerous previously identified polar genes (e.g. Ly6a, Gsto1, Ddah1, Utf1, B4galt6, Cpne3, Duox2, Nat8l, Pou3f1, Ppp2r2c, Rhox5, Rrm2, Sorl1 or Top2a, Sup. Fig. 5). On the contrary, the subpopulation with high pseudotime values expressed differentiation markers Flt1, Krt8, Krt18, Ndrg1, Basp1, Ctsb or Slc5a5 (Shi et al., 2013; Sood et al., 2006b). The expression of these genes was confirmed in the blastocysts by comparing the expression in polar and mural TE cells (Fig. 4I)(Nakamura et al., 2015).

Differential genes expression between the two subpopulations also suggested a number of new putative markers (Fig. 4H). Using smFISH, we confirmed that Ly6a, whose expression was increased in LT21 TSCs, was indeed more prominently expressed in the polar cells of blastocysts (3/3, Sup. Fig. 4I) and of blastoids (7/10, Sup. Fig. 4J). Of note, Ly6a was also previously proposed to mark stem cells in E8.5 placentas (Natale et al., 2017). Altogether, we concluded that inductive signals originating from the embryonic compartment regulate trophoblast gene expression and self-renewal, and contribute to the polar to mural patterning of the trophectoderm (Figure 5). Combined, these embryonic inductive signals regulate aspects of polar trophoblasts and of trophectoderm patterning *in vitro*.

Material and methods:

Cell culture: TSC are cultured under Tx conditions followed a previously published protocol (Kubaczka et al., 2014). After coating with Matrigel, cells are cultured in Tx media, which consists of phenol red free DMEM/F12 supplemented (phenol red-free, with l-glutamine), insulin (19.4 µg/ml), l-ascorbic-acid-2-phosphate (64 µg/ml), sodium selenite (14 ng/ ml), insulin (19.4 µg/ml), sodium bicarbonate (543 µg/ml), holo-transferrin (10.7 µg/ml), penicillin streptomycin, FGF4 (25 ng/ml), TGFβ1 (2 ng/ml) and heparin (1 µg/ml). LT21 cultured cells were plated in laminin 521 coated plates (10 ug/ml diluted in PBS with Mg2+ and Ca2+) using Tx media supplemented with Il11 (50 ng/ml), Activin (50ng/ml), Bmp7 (25 ng/ml), LPA (5 nM) and 8Br-cAMP (200 nM). TSCs were differentiated by refreshing with plain TX media without Fgf4, Tgfb1 nor any other CDX2 regulator. This media was maintained for 6 days. ESC were cultured under 2i conditions (Ying et al., 2008) in gelatin coated plates. Cells were routinely passaged using trypsin and quenched with trypsin soybean inhibitor.

TSC line derivation: E3.5 blastocysts were isolated from pregnant females. Zona pellucida was removed using Tyrode acid solution and then they were placed in MEF coated plates in the presence of Tx or Tx21 media. Media was carefully changed every 48h. The outgrowth was monitored daily and was passaged on day 4 or 5 depending on cell growth. Cultures including Tx21 were passaged into MEF coated plates for one more passage since this facilitates attachment of the single cells. Only in passage 3 they would be converted to LT21 cultures being plated in laminin 521 pre-coated plates.

bioRxiv preprint doi: https://doi.org/10.1101/510362; this version posted January 3, 2019. The copyright holder for this preprint (which was not certified by peer review) is the author/funder. All rights reserved. No reuse allowed without permission.

Cell cycle analysis: After trypsinization, 10E5 TSCs and plTSCs were incubated in 0.5ml of Tx media with 10 ug/ml hoescht 34580 for 30 minutes at 37C. After the incubation time, tubes with cells were placed on ice and analyzed with a FACSCanto II.

Colony formation assay: Single cells were sorted in MEF coated plates in the presence of either Tx or LT21 media. Media was changed every 48 hours and the number of wells containing colonies was assessed 7 days after sorting.

Chimera formation: After blastocyst isolation from pregnant females, a micromanipulator was used for injecting 10 TSCs in the blastocyst cavity. Those blastocysts were then implanted in one of the uterine horns of pseudopregnant females. Each female had only one of their horns used for implantation and a maximum of 8 blastocysts were used per female. Placenta isolation was performed at E.10.5 (time of implantation was considered as 3.5). Histology was performed on the GFP imaged placentas using an antibody against GFP.

Immunofluorescence: Samples were fixed using 4%PFA in PBS for 20 minutes at RT followed by 3 washing steps with PBS. A 0.25% triton solution in PBS was used for permeabilization during 30 minutes ar RT,followed by a 1 hour blocking step with PBS+ 10% FBS and 0.1% tween20. Primary antibodies against CDX2 (Biogenes MU392A-5UC), EOMES (Abcam ab23345), ZO-1 (Fisher scientific # 33-9100), Krt8/18 (DAKO M365201-2), GATA6 (R&D AF1700) or ECADHERIN (life technologies # 14-3249-82) were diluted 1/200 in PBS + 0.1% Tween20, and used for staining O/N at 4C. After three washing steps, samples were incubated with the corresponding secondary antibodies for 1 hour at RT. Hoechst was used for counterstaining with or withouth WGA. All images were analyzed in a PerkinElmer Ultraview VoX spinning disk microscope.

single molecule FISH: TSCs plated in glass coverslips were allowed to grow and were then fixed using RNAse free 4%PFA in PBS + 1% Acetic Acid during 20 minutes. After fixation, all samples followed the Quantigene ViewRNA kit instructions: After three washes with RNAse free PBS, samples were incubated for 10 minutes in a detergent solution. After three washes with RNAse free PBS, samples were incubated for 5 minutes at RT with Q protease. After three washes with RNAse free PBS, samples were incubated at 40C for 3 hours (in a humidified chamber) with the probes of interest diluted in Probe set diluent. After 3 washes with wash buffer, samples were incubated at 40C for 30 minutes with preamplifier diluted in amplifier diluent. After 3 washes with wash buffer, samples were incubated at 40C for 30 minutes with amplifier diluted in amplifier diluent. After 3 washes with wash buffer, samples were incubated at 40C for 30 minutes with label diluted in label probe diluent. After 2 washes with wash buffer, they were washed once more for 10 minutes. Samples were then incubated for 15 minutes in RNAse free PBS with Hoechst and WGA as counterstains followed by 3 washes with RNAse free PBS. Blastocysts were carefully placed in mounting media in glass bottom 3.5 mm plates. All samples were imaged with a 63x oil immersion objective in a PerkinElmer Ultraview VoX spinning disk microscope.

High content imaging: Each colony was imaged for E-CADHERIN, CDX2, EOMES and Nuclei stainings. E-CADHERIN staining was used for manual cell segmentation in ImageJ. Cell profiler was used for analysis of cells segmentation and the other stainings. Measurements obtained in Cell Profiler were used for further analysis using a Python pipeline. After discarding dividing cells based on the nuclear staining, a total of 502 control cells and 297 plTSCs cells were analyzed.

RNA sequencing: For bulk sequencing 1000 control and LT21 cultured cells were used for Trizol extraction RNA extraction from both bulk and single cells was performed following the Cel Seq 2 protocol (Hashimshony et al., 2016). Bulk samples were first normalized and then analyzed using the DESeq2 package on Rstudio. Triplicates for each group (F4 in Tx, F4 in LT21, F4 in Tx differentiated, F4 in LT21 differentiated) were analyzed. Differentially expressed were those showing an upregulation of 1.5 fold change with a p value lower than 0.05. DAVID gene onthology online tool was used for gene enrichment analysis.

bioRxiv preprint doi: https://doi.org/10.1101/510362; this version posted January 3, 2019. The copyright holder for this preprint (which was not certified by peer review) is the author/funder. All rights reserved. No reuse allowed without permission.

smFISH polarity quantification: Confocal images were taken with a z-step of 0.3 µm. Given the complexity of an analysis performed in 3 dimensions that would require an algorithm capable of segmenting cells and quantifying the number of transcripts in 3D, we decided to quantify a 2 dimension projection of the slices that included the ICM and blastocoel. Those z-stack projections were oriented with polar side at the left and mural side at the right and they were then analyzed for average column pixel intensity, allowing us to plot an average pixel intensity histogram. An intensity profile was plotted for each embryo and gene. Each blastocyst is structurally different showing distinct cavity sizes, which implies that a different percentage of the TE is in contact with the ICM for each embryo. In order to compare the expression of polar and mural TE, we divided the length of the embryo in three segments of equal distance, irrespective of the total diameter. The intermediate segment was considered a transition stage between the polar and mural regions and therefore was not included in the next analyses. The polar and mural segments of the profile were analyzed by comparing the average pixel intensities of each pixel column included in the segment.

Blastoid formation: Full protocol link: https://www.nature.com/protocolexchange-/protocols/6579) Agarose microwell arrays were casted using the PDMS stamp and incubated O/N on mES serum containing media. After washing the chips with PBS, a ESC solution of 8000 cells/150 µl is dispensed in the central chip are and allowed to settle. After 15 minutes, an additional 1ml is dispensed. 20 hours later 1 ml of media is removed and a TSC solution of 22000 cells/150 ul is dispensed. After allowing the cells to fall in the microwells, 1 ml of blastoid media is added to the wells. Blastoid media includes 20 µM Y27632 (AxonMed 1683), 3 uM CHIR99021 (AxonMed 1386), 1 mM 8Br-cAMP (Biolog Life Science Institute B007E), 25 ng/ml Fgf4 (R&D systems 5846F4), 15 ng/ml Tgfb1 (Peprotech 100-21), 30 ng/ml Il11 (Peprotech 200-11) and 1 µg/ml heparin (Sigma-Aldrich cat# H3149). An additional dose of cAMP is dispensed 24 hours after TSC seeding. All measurements are performed 65 hours after TSC seeding.

Gardner, R.L. (2000). Flow of cells from polar to mural trophectoderm is polarized in the mouse blastocyst. Hum. Reprod. *15*, 694–701.

Guillemot, F., Nagy, A., Auerbach, A., Rossant, J., and Joyner, A.L. (1994). Essential role of Mash-2 in extraembryonic development. Nature *371*, 333–336.

Hirashima, M., Lu, Y., Byers, L., and Rossant, J. (2003). Trophoblast expression of fms-like tyrosine kinase 1 is not required for the establishment of the maternal-fetal interface in the mouse placenta. Proc. Natl. Acad. Sci. U. S. A. *100*, 15637–15642.

Hutchens, S.A., León, R.V., O'neill, H.M., and Evans, B.R. (2007). Statistical analysis of optimal culture conditions for Gluconacetobacter hansenii cellulose production. Lett. Appl. Microbiol. *44*, 175–180.

Imakawa, K., Dhakal, P., Kubota, K., Kusama, K., Chakraborty, D., Karim Rumi, M.A., and Soares, M.J. (2016). CITED2 modulation of trophoblast cell differentiation: insights from global transcriptome analysis. Reproduction *151*, 509–516.

Kuales, G., Weiss, M., Sedelmeier, O., Pfeifer, D., and Arnold, S.J. (2015). A Resource for the Transcriptional Signature of Bona Fide Trophoblast Stem Cells and Analysis of Their Embryonic Persistence. Stem Cells Int. *2015*, 218518.

Kubaczka, C., Senner, C., Araúzo-Bravo, M.J., Sharma, N., Kuckenberg, P., Becker, A., Zimmer, A., Brüstle, O., Peitz, M., Hemberger, M., et al. (2014). Derivation and maintenance of murine trophoblast stem cells under defined conditions. Stem Cell Reports *2*, 232–242.

bioRxiv preprint doi: https://doi.org/10.1101/510362; this version posted January 3, 2019. The copyright holder for this preprint (which was not certified by peer review) is the author/funder. All rights reserved. No reuse allowed without permission.

Latos, P.A., Goncalves, A., Oxley, D., Mohammed, H., Turro, E., and Hemberger, M. (2015). Fgf and Esrrb integrate epigenetic and transcriptional networks that regulate self-renewal of trophoblast stem cells. Nat. Commun. *6*, 7776.

McDole, K., and Zheng, Y. (2012). Generation and live imaging of an endogenous Cdx2 reporter mouse line. Genesis *50*, 775–782.

Menchero, S., Rayon, T., Andreu, M.J., and Manzanares, M. (2017). Signaling pathways in mammalian preimplantation development: Linking cellular phenotypes to lineage decisions. Dev. Dyn. *246*, 245–261.

Morioka, Y., Nam, J.-M., and Ohashi, T. (2017). Nik-related kinase regulates trophoblast proliferation and placental development by modulating AKT phosphorylation. PLoS One *12*, e0171503.

Moriwaki, K., Tsukita, S., and Furuse, M. (2007). Tight junctions containing claudin 4 and 6 are essential for blastocyst formation in preimplantation mouse embryos. Dev. Biol. *312*, 509–522.

Motomura, K., Oikawa, M., Hirose, M., Honda, A., Togayachi, S., Miyoshi, H., Ohinata, Y., Sugimoto, M., Abe, K., Inoue, K., et al. (2016). Cellular Dynamics of Mouse Trophoblast Stem Cells: Identification of a Persistent Stem Cell Type. Biol. Reprod. *94*, 122.

Nakamura, T., Yabuta, Y., Okamoto, I., Aramaki, S., Yokobayashi, S., Kurimoto, K., Sekiguchi, K., Nakagawa, M., Yamamoto, T., and Saitou, M. (2015). SC3-seq: a method for highly parallel and quantitative measurement of single-cell gene expression. Nucleic Acids Res. *43*, e60.

Rivron, N. (2018). Formation of blastoids from mouse embryonic and trophoblast stem cells.

Rivron, N., Pera, M., Rossant, J., Martinez Arias, A., Zernicka-Goetz, M., Fu, J., van den Brink, S., Bredenoord, A., Dondorp, W., de Wert, G., et al. (2018a). Debate ethics of embryo models from stem cells. Nature *564*, 183–185.

Rivron, N.C., Frias-Aldeguer, J., Vrij, E.J., Boisset, J.-C., Korving, J., Vivié, J., Truckenmüller, R.K., van Oudenaarden, A., van Blitterswijk, C.A., and Geijsen, N. (2018b). Blastocyst-like structures generated solely from stem cells. Nature *557*, 106–111.

Shi, X.-H., Larkin, J.C., Chen, B., and Sadovsky, Y. (2013). The expression and localization of N-myc downstream-regulated gene 1 in human trophoblasts. PLoS One *8*, e75473.

Sood, R., Kalloway, S., Mast, A.E., Hillard, C.J., and Weiler, H. (2006a). Fetomaternal cross talk in the placental vascular bed: control of coagulation by trophoblast cells. Blood *107*, 3173–3180.

Sood, R., Zehnder, J.L., Druzin, M.L., and Brown, P.O. (2006b). Gene expression patterns in human placenta. Proc. Natl. Acad. Sci. U. S. A. *103*, 5478–5483.

Tanaka, S., Kunath, T., Hadjantonakis, A.K., Nagy, A., and Rossant, J. (1998). Promotion of trophoblast stem cell proliferation by FGF4. Science *282*, 2072–2075.

Trapnell, C., Cacchiarelli, D., Grimsby, J., Pokharel, P., Li, S., Morse, M., Lennon, N.J., Livak, K.J., Mikkelsen, T.S., and Rinn, J.L. (2014). The dynamics and regulators of cell fate decisions are revealed by pseudotemporal ordering of single cells. Nat. Biotechnol. *32*, 381–386.

Zhang, H.T., and Hiiragi, T. (2018). Symmetry Breaking in the Mammalian Embryo. Annu. Rev. Cell Dev. Biol. *34*, 405–426.

Zhang, H.T., and Hiiragi, T. (2018). Symmetry Breaking in the Mammalian Embryo. Annu. Rev. Cell Dev. Biol. *34*, 405–426.

bioRxiv preprint doi: https://doi.org/10.1101/510362; this version posted January 3, 2019. The copyright holder for this preprint (which was not certified by peer review) is the author/funder. All rights reserved. No reuse allowed without permission.

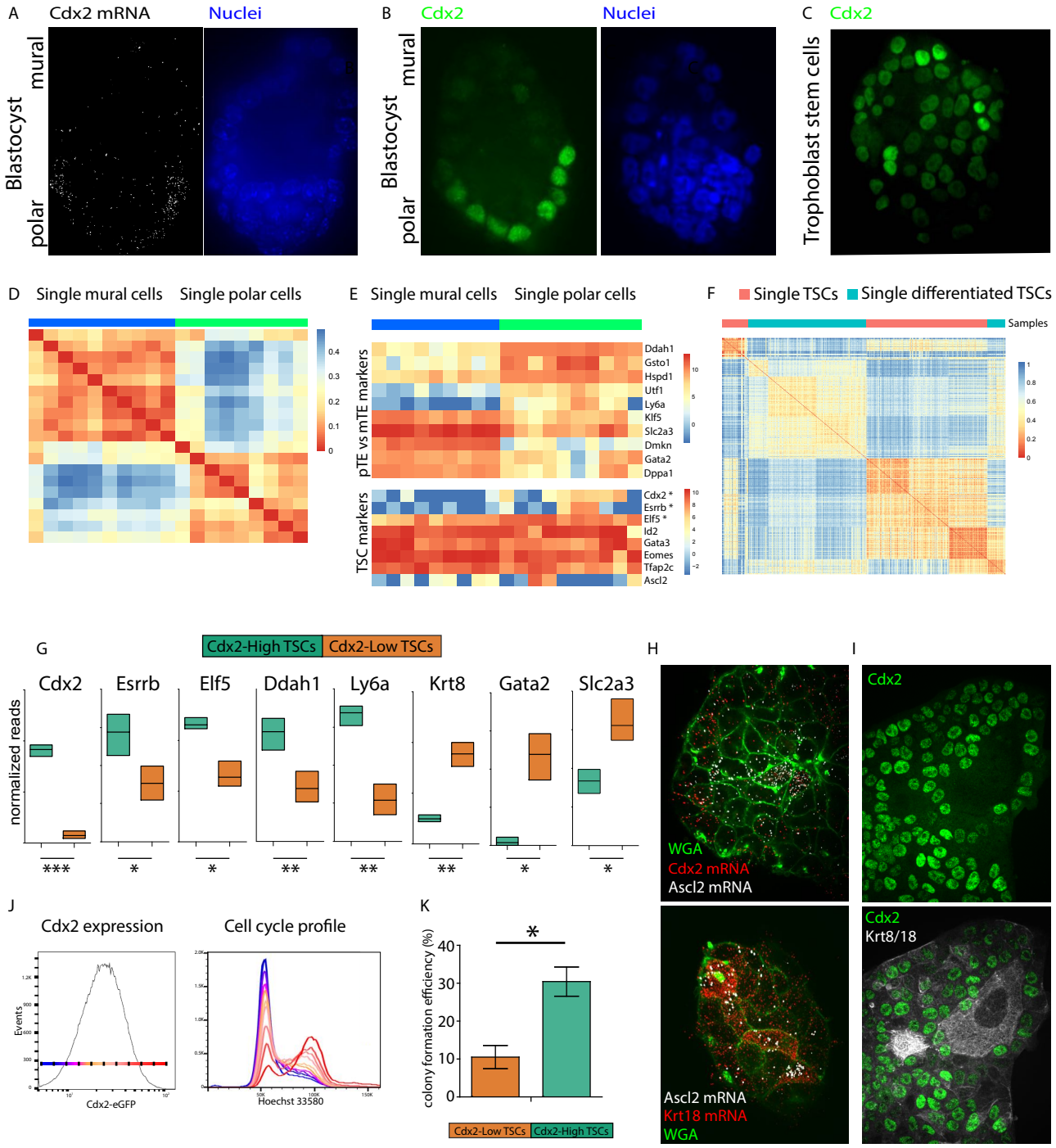

Figure 1. A. smFISH for Cdx2 mRNA on E4.5 blastocysts. B. CDX2 protein detection in E3.75 blastocyst after being cultured for 6 hours in plain M2 media. C. Heterogeneous expression of CDX2 in cultured TSCs. D.Unsupervised gene clustering analysis of E4.5 trophectoderm single cells (Nakamura et al.). E. Gene expression heatmap for TE single cells. F. Unsupervised gene clustering analysis of control TSCs and 6 day differentiated TSCs. G. Differential gene expression of differentiation markers in CDX2-High and CDX2-Low populations. * for pvalue<0.05, ** for pvalue< 0.01 and *** for pvalue<0.001. H. smFISH for Cdx2 and Ascl2 transcripts in TSCs (top) or for Ascl2 and Krt18 (bottom). I. Anticorrelation found on TSCs for CDX2 and Krt8/18 expression as assessed by immunofluorescence. J. Cell cycle analysis of TSCs cultures shows a correlation between CDX2 expression and Cell cycle state. I. Colony formation potential of single CDX2-High and CDX2-Low cells. fc=2.89, pvalue=0.015.

bioRxiv preprint doi: https://doi.org/10.1101/510362; this version posted January 3, 2019. The copyright holder for this preprint (which was not certified by peer review) is the author/funder. All rights reserved. No reuse allowed without permission.

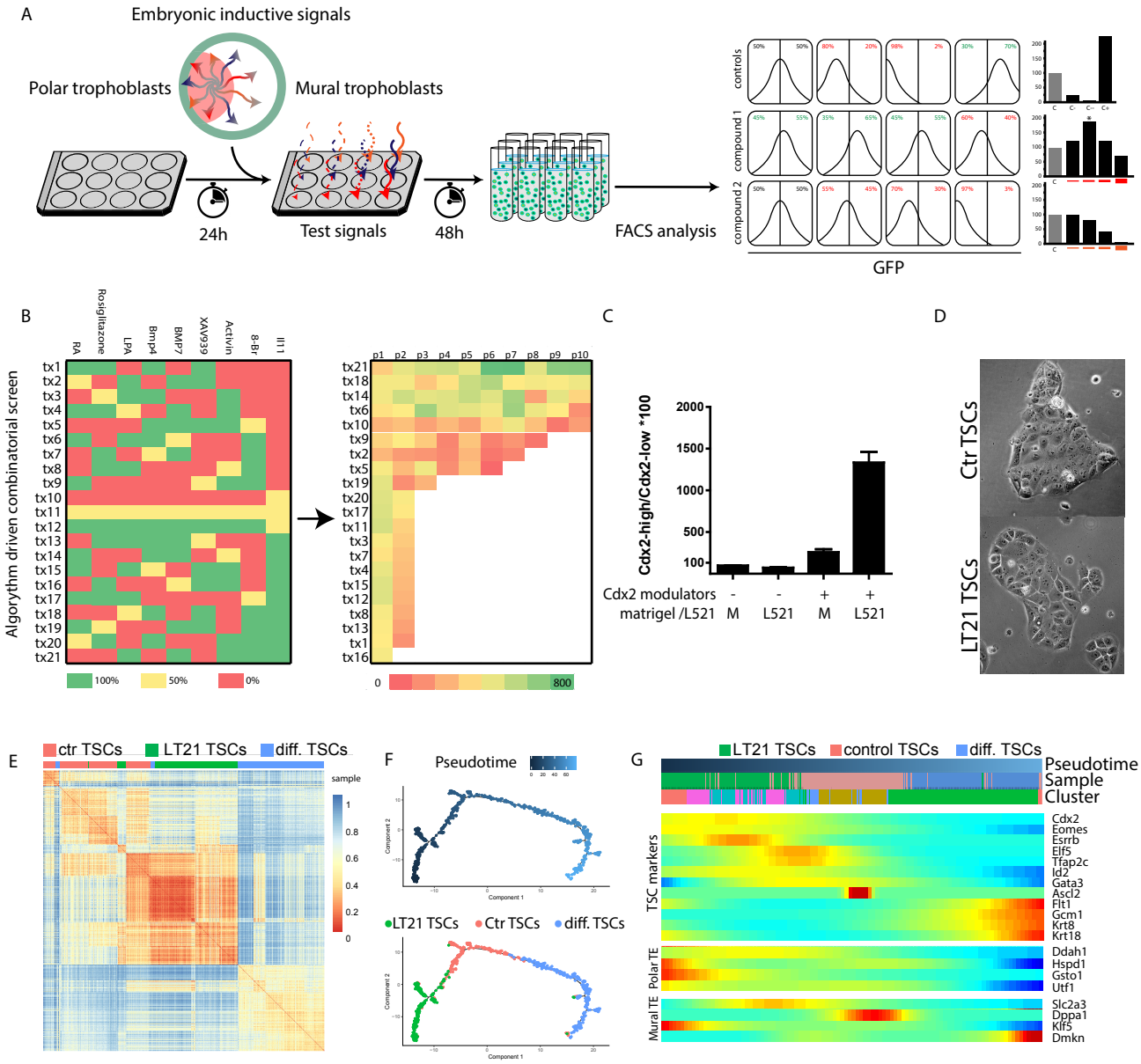

Figure 2. A. Strategy followed in order to identify CDX2 expression regulators in CDX2-eGFP TSCs. B. List of 21 different cocktails combining the 9 different CDX2 regulators. On the right panel the 21 cocktails are sorted based on the average CDX2-High/ CDX2-Low ratio. C. Comparative CDX2-High/CDX2-Low ratio of TSCs upon combination of CDX2 regulators with Laminin521. D. Bright field microscopy pictures of TSCs colonies cultured in control or LT21 cultures. E. Unsupervised gene clustering analyisis performed on single cells from LT21, control and differentiated cultures. F. Single cell pseudotime trajectory obtained from monocle. G. Pseudotime heatmap for visualization of expression peaks for polar, mural and classical TSC markers.

bioRxiv preprint doi: https://doi.org/10.1101/510362; this version posted January 3, 2019. The copyright holder for this preprint (which was not certified by peer review) is the author/funder. All rights reserved. No reuse allowed without permission.

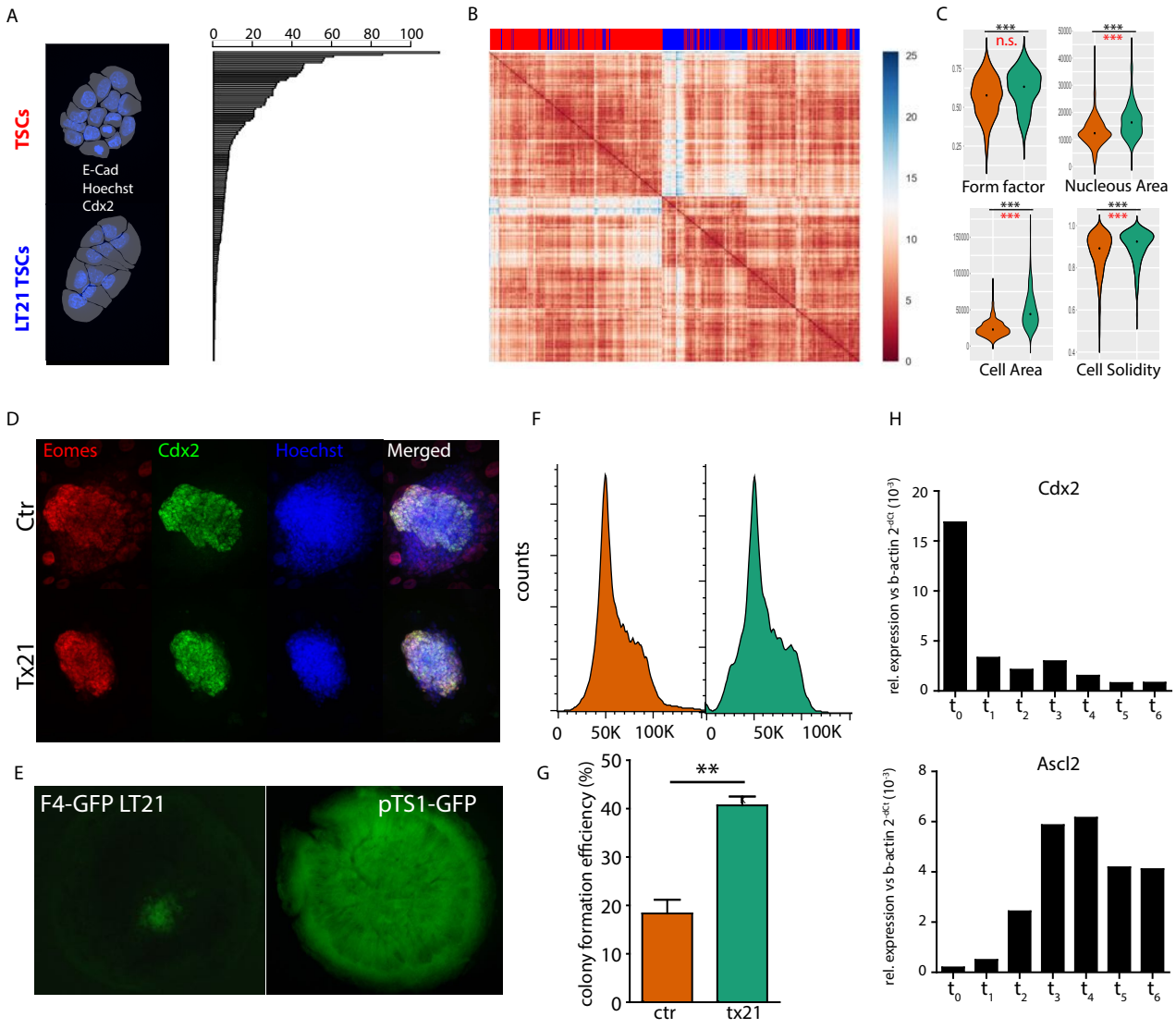

Figure 3. A. Morphological feature extraction after cell segmentation based on e-cadherin staining. Differential features were ranked based on their pvalue after Mann-Whitney statistical analysis. B. Clustering based on the top 20% differential features. A cluster includes the majority of LT21 TSCs (blue) and some control TSCs (red). C. Violin plots representing the value distribution for some of the top ranked differential features. Unpaired two-tailed t test (black) and F test for variance (red). ***=pvalue<0.001. D. CDX2 and EOMES staining of blastocyst outgrowths 4 days after plating. E. Isolatted E10.5 placentas after blastocyst injection using F4 GFP LT21 TSCs or pTS1 (directly derived in Tx21/LT21 conditions). F. Cell cycle analysis of control (orange) and LT21 TSCs (green). G. Colony formation efficiency of single sorted control (orange) or LT21 TSCs (green). H. Differentiation dynamics of LT21 TSCs upon removal of all CDX2 regulators. A sample was taken every 24 hours after compound removal at t0.

bioRxiv preprint doi: https://doi.org/10.1101/510362; this version posted January 3, 2019. The copyright holder for this preprint (which was not certified by peer review) is the author/funder. All rights reserved. No reuse allowed without permission.

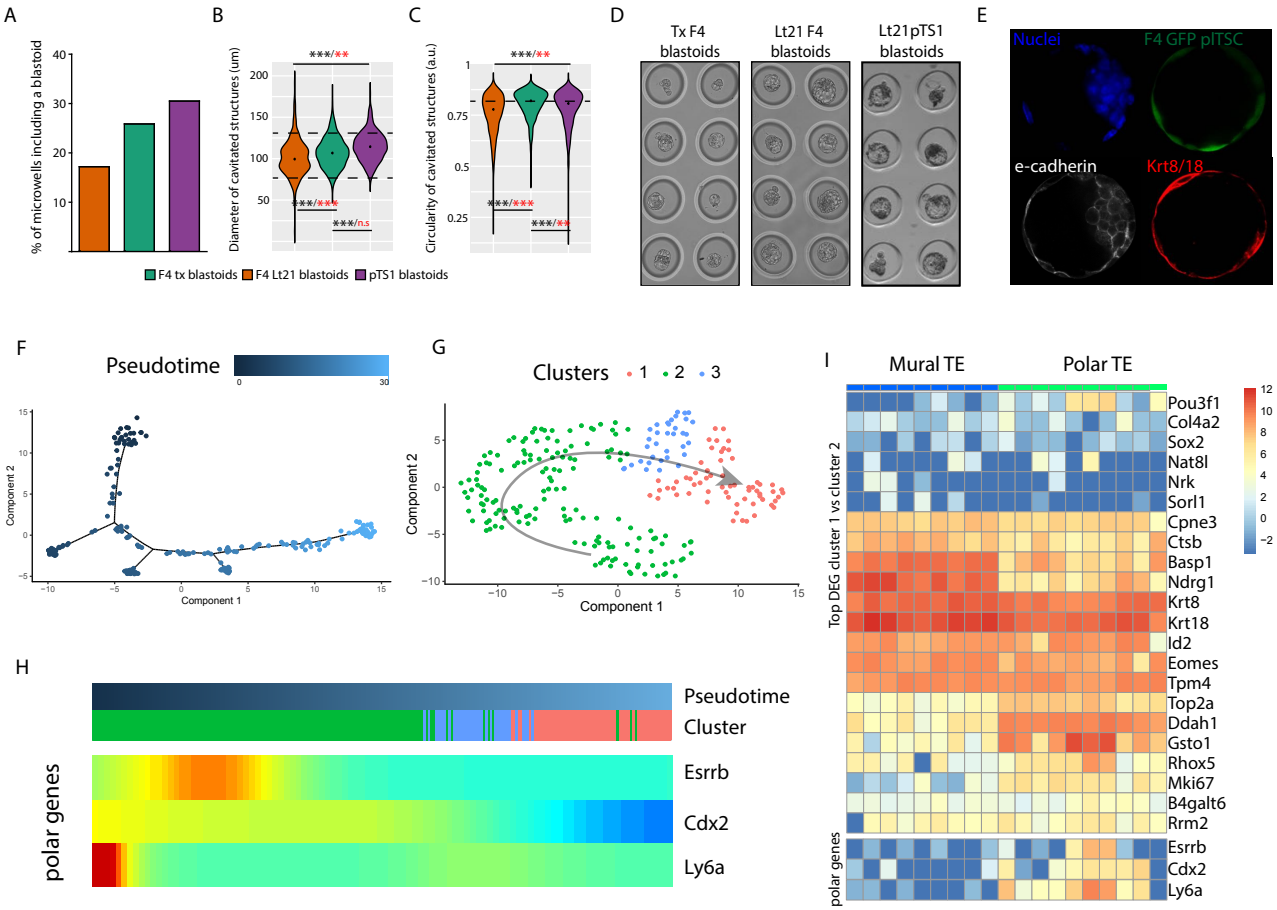

Figure 4. A. Percentage of microwells including a blastoid (correct circularity, diameter and presence of one single cavity). Comparison of control TSCs (F4, green) and LT21 TSCs (F4 converted to LT21 in green; pTS1 directly derived in LT21 conditions in purple). B. Diameter of all structures included in the microwells. C. Circularity of all structures included in the microwells. Two-tailed unpaired t-test. ** for pvalue<0.01, *** for pvalue<0.001. Black for analysis of the means, red for F variance. D. Representative pictures of microwells including control F4, LT21 F4, and pTS1 blastoids. E. Blstoid obtained using LT21 F4 TSCs stained for E-CADHERIN and KRT8/18. F. Pseudotime trajectory of single cells isolated from blastoids. G. Clustering analysis from monocle groups the cells in three different clusters. H. Pseudotime heatmap for the genes Esrrb and Cdx2, which suggest cluster 2 to be more undifferentiated. Ly6a shows a clear expression peak at low pseudotime values and ahigher expresion in cluster 2. I. After differential gene expression between clsuters 1 and 2, the top 25 differentially expressed genes were plotted for the single cells obtained from the polar and mural TE of E4.5 blastocysts.

bioRxiv preprint doi: https://doi.org/10.1101/510362; this version posted January 3, 2019. The copyright holder for this preprint (which was not certified by peer review) is the author/funder. All rights reserved. No reuse allowed without permission.

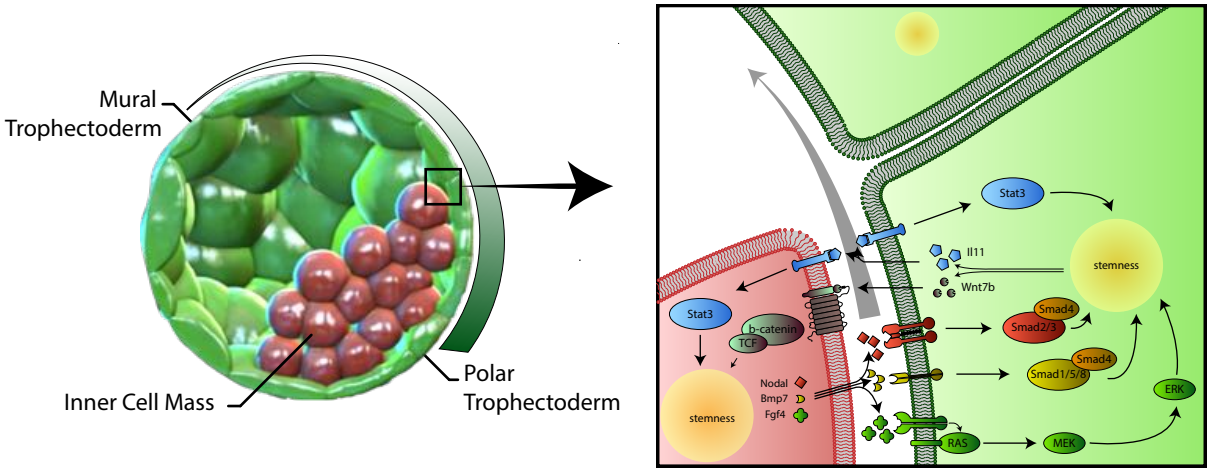

Figure 5. Active communication between both compartments takes place, being the potency of the trophectoderm dependent on embryonic signals. As the cells in the TE proliferate, the mural TE distances from the ICM becoming less exposed to its signals, resulting in differentiation of the mural TE cells while the polar TE conserves the stem cell pool.

bioRxiv preprint doi: https://doi.org/10.1101/510362; this version posted January 3, 2019. The copyright holder for this preprint (which was not certified by peer review) is the author/funder. All rights reserved. No reuse allowed without permission.

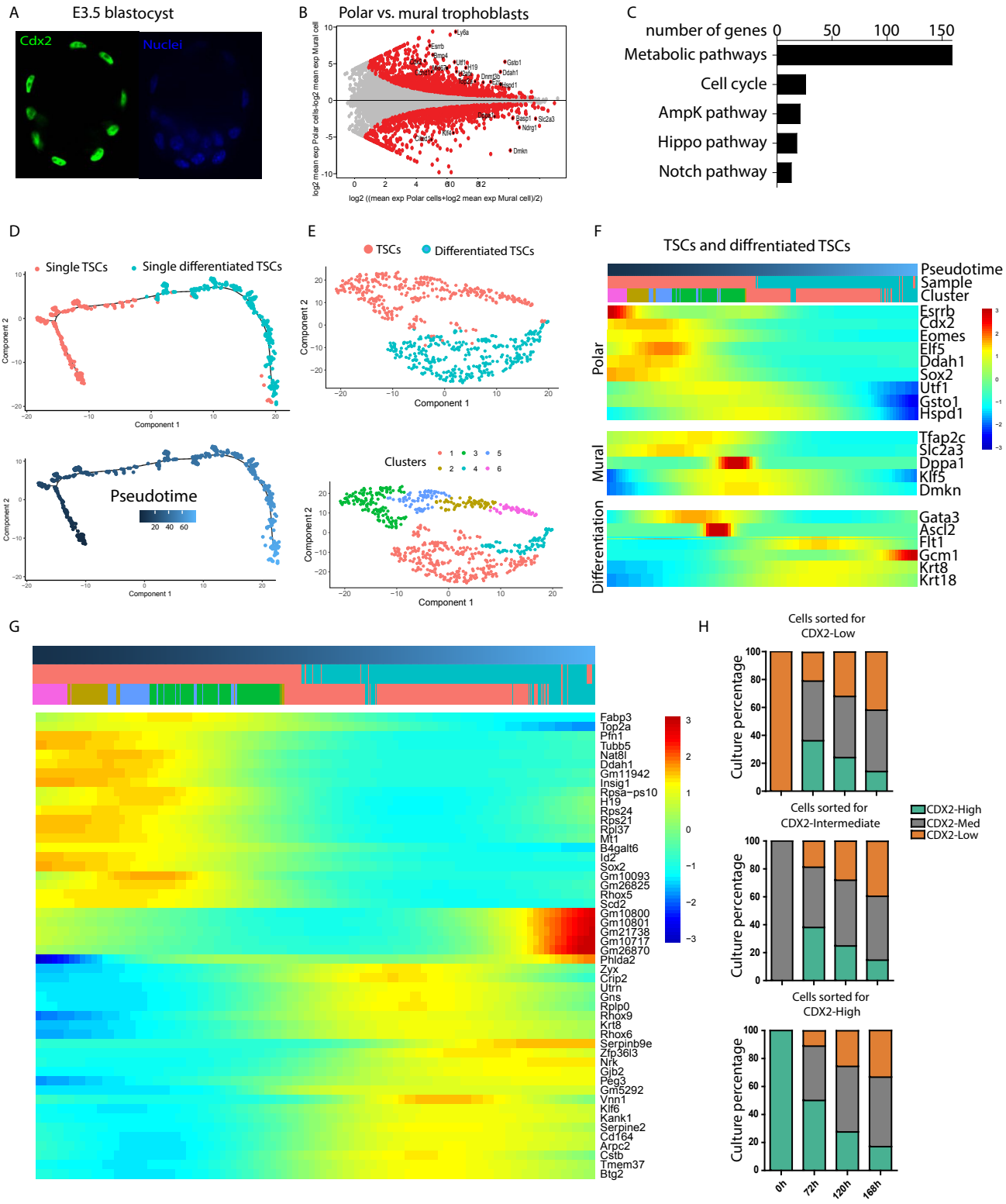

Supplementary figure 1. A. CDX2 staining on freshly isolated E3.5 blastocysts. B. Differential gene expression between mural and polar cells isolated from the TE of E4.5 blastocysts (Nakamura et al.). C. GO Pathway enrichement based on differential gene expression analysis of CDX2-High and CDX2-Low samples. D. control TSCs and differentiated TSCs were located in a pseudotime trajectory by Monocle. E. Clustering analyisis of control TSCs and differentiated TSCs. F. Expression peaks for polar, mural and differentiation markers. G. Top 50 genes defining the pseudotime trajectory. H. Percentage of the different subpopulations upon pure subpopulation sorting and further independent culture.

bioRxiv preprint doi: https://doi.org/10.1101/510362; this version posted January 3, 2019. The copyright holder for this preprint (which was not certified by peer review) is the author/funder. All rights reserved. No reuse allowed without permission.

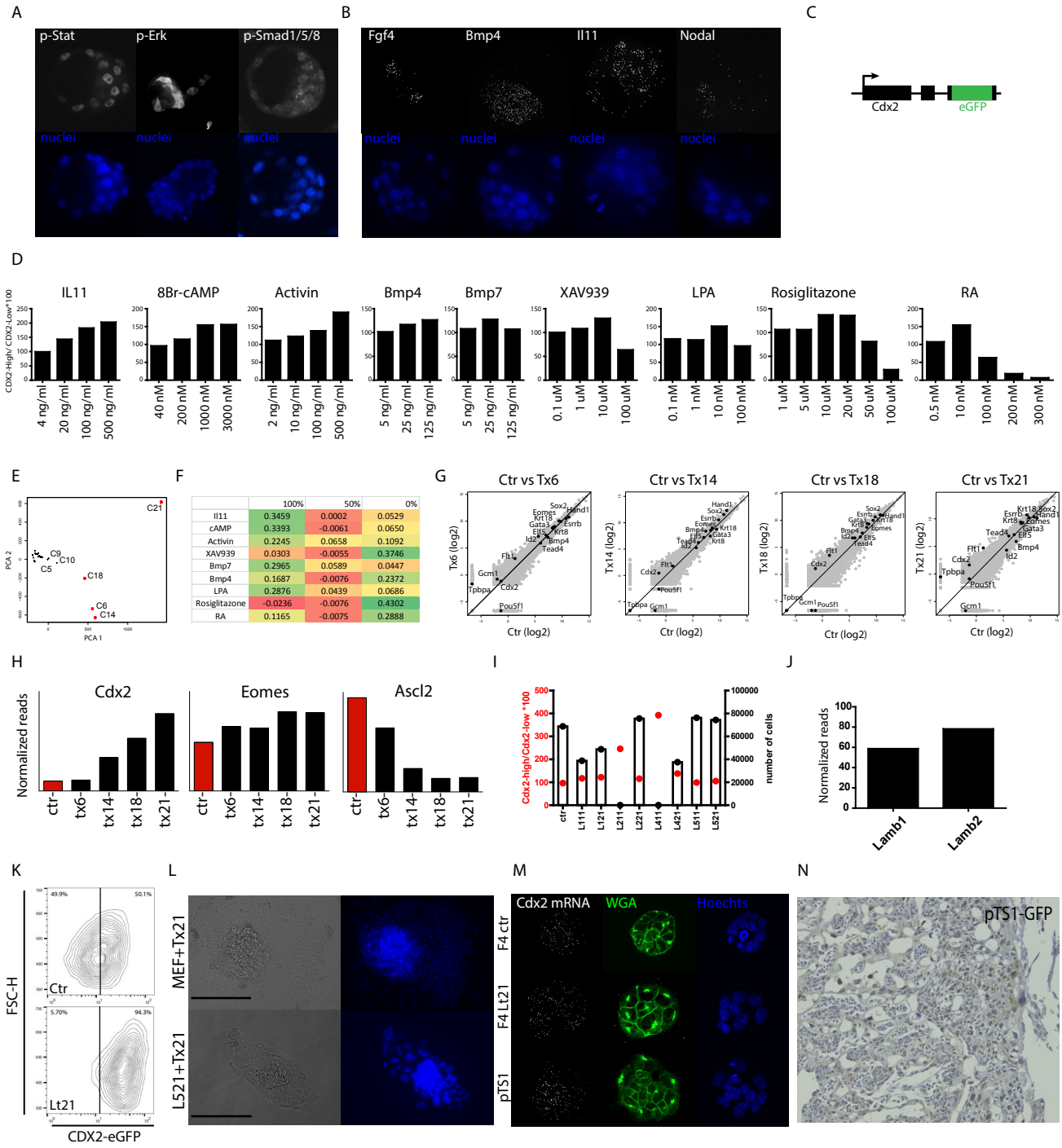

Supplementary figure 2. A. Pathway activation stainings performed in freshly isolated E3.5 blastocysts. B. smFISH performed on freshly isolated blastocysts allow us to detect expression of key pathway ligands. C. Cdx2 locus of CDX2-eGFP TSCs. D. Positive CDX2 expression modulators induce a higher expression of CDX2 in a dose-dependent manner. E-F. Principal component analysis suggest the effect on CDX2 expression of each compound at a given concentration. G. Bulk transcriptome analysis allows us to compare the overall expression of key trophoblast markers fr each culture condition. H. Expression of the Cdx2 and Eomes (as un-differentiated markers) and Ascl2 (as a partially differentiated marker) across the 4 best cultures. I. CDX2 expression and proliferation quantification of TSCs cultured in control conditions on plates coated with different laminins. J. Lamb1 and Lamb2 expression levels in bulk samples from blastocysts. K. Tx21 compounds combined with L521 dramatically increase the percentage of CDX2-High cells without affecting the size of the cells. L. Proliferation comparison of trophoblasts 4 days after blastocyst plating on either mEF or L521. M. Newly derived cell TS lines grow in colonies and express Cdx2. N. Staining against GFP on tissue sections obtained from placentas showing TSC contribution.

bioRxiv preprint doi: https://doi.org/10.1101/510362; this version posted January 3, 2019. The copyright holder for this preprint (which was not certified by peer review) is the author/funder. All rights reserved. No reuse allowed without permission.

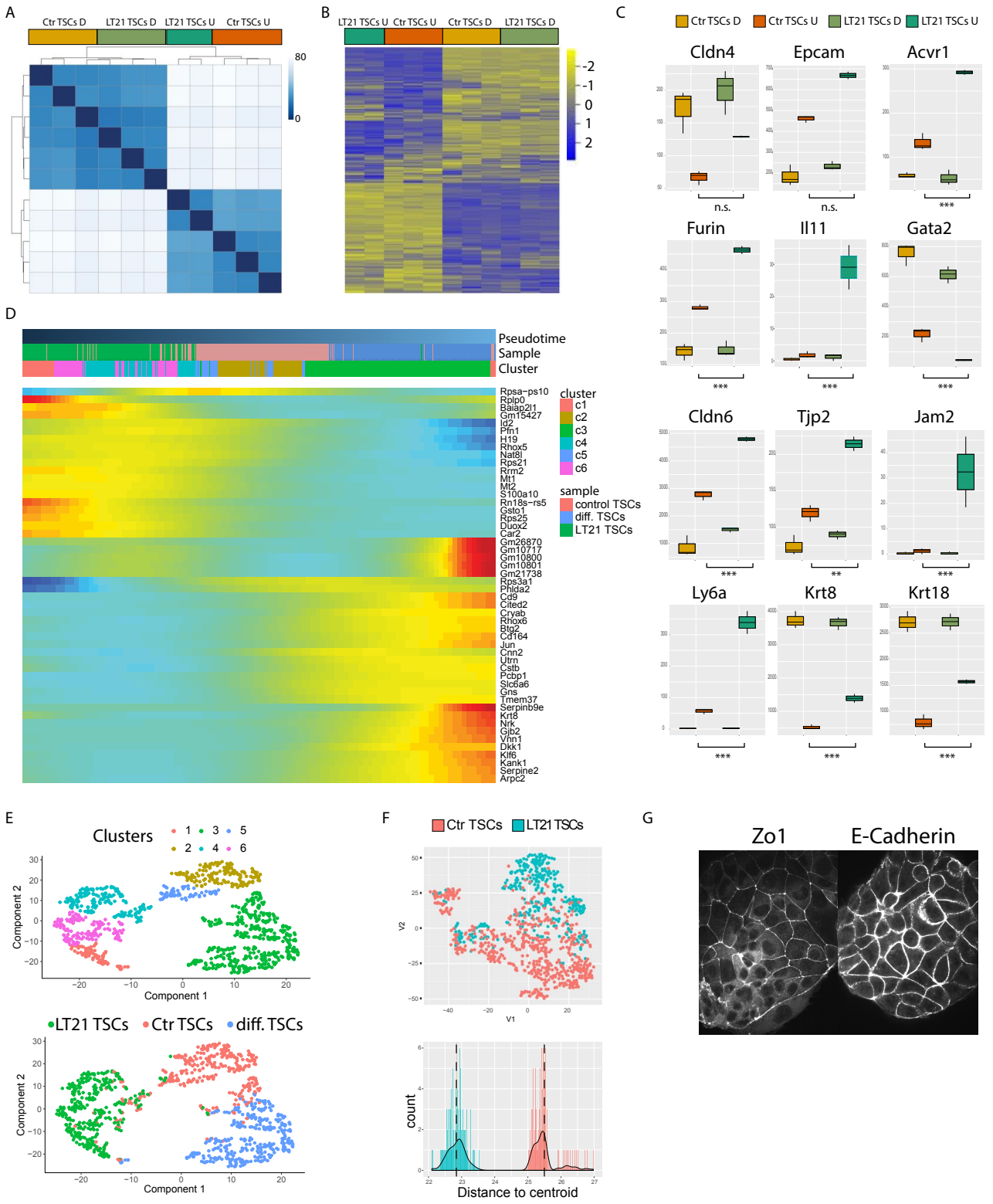

Supplementary Figure 3. A. Unsupervised gene clustering of differentiated and undifferentiated control and LT21 cultures of TSCs. B. Heatmap showing differenially expressed genes across samples. C. Different expression levels for genes important for the differentiation or epithelial state. D.Top 50 genes defining the pseudotime trajectory. E. Monocle clustering analyisis of single cells from LT21, control and differentiated samples. F. Representative t-SNE map plotting each cell based on the morphological features extracted (top) and average distance to centroid for control (red) and LT21 cultured TSCs (blue). H. Expression of E-cadherin and ZO1 in LT21 cultured TSCs.

bioRxiv preprint doi: https://doi.org/10.1101/510362; this version posted January 3, 2019. The copyright holder for this preprint (which was not certified by peer review) is the author/funder. All rights reserved. No reuse allowed without permission.

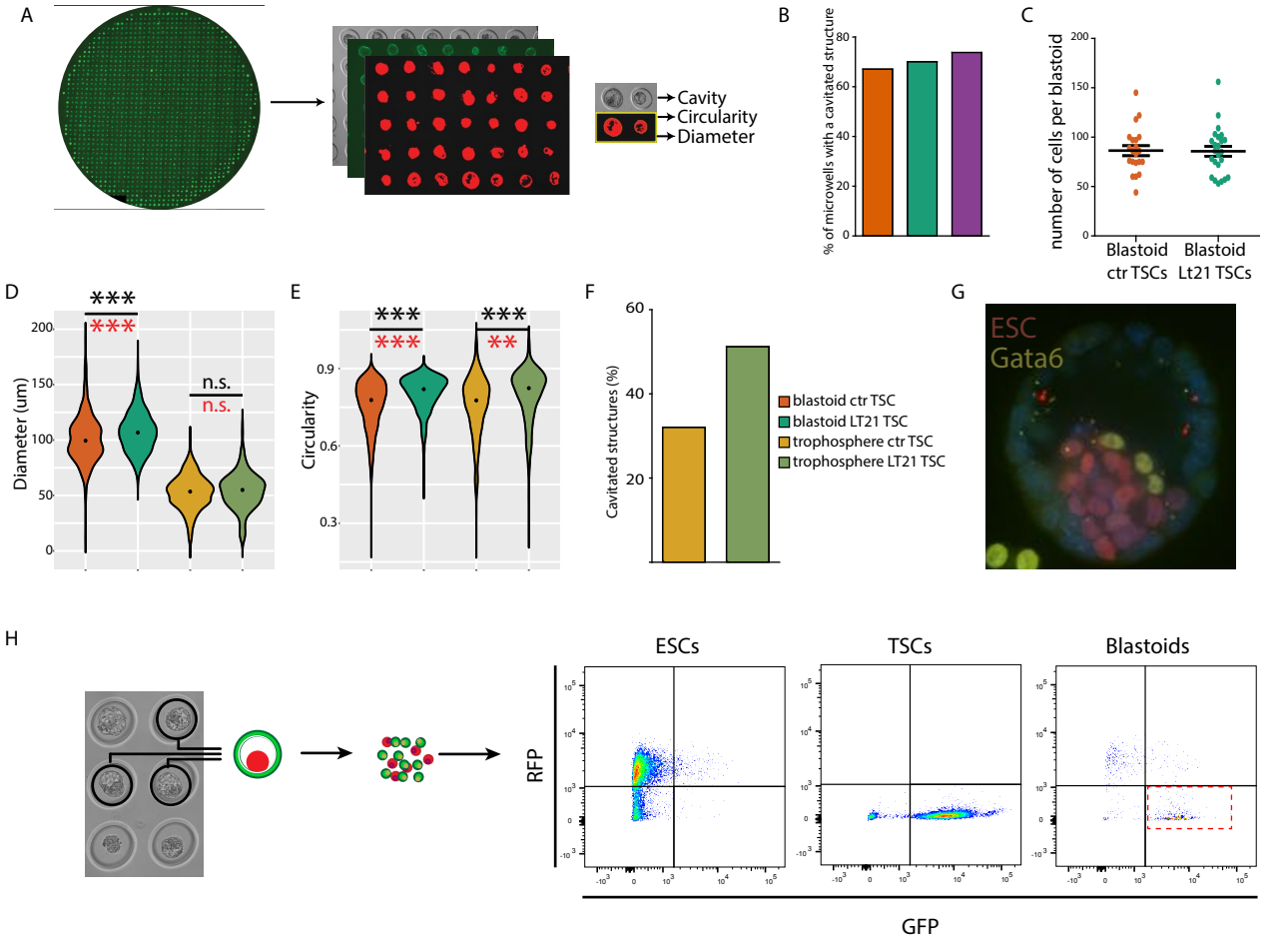

Supplementary figure 4. A. Imaging of agarose microwells with bright field and fluorescence microscopy after staining with WGA. Stained membranes allow us to perform a semi-automated acquisition of morphological parameters. B. Percentage of microwells with a cavitated structure across cultures. C. Diameter of all structures for control and LT21 F4 TSCs, both as blastoids and trophospheres. D. Circularity of all structures for control and LT21 F4 TSCs, both as blastoids and trophospheres. E. Percentage of cavitated structures obtained from control and LT21 F4 TSCs. F. Blastoid obtained from LT21 F4 TSCs stained for GATA6. G. Aproach for blastoid single trophoblast isolation. After selection of blastoids, these are digested and single GFP+ cells are sorted. H-I. smFISH staining for Ly6a on E3.5 blastocysts allows for projection of the multiple Z-steps allowing us to quantify intensity . Only Z-steps including a large portion of the blastocoel were included in the projection. All projections are measured in a polar-to-mural orientation. The length of the projection was divided into a polar third, a mural third and an intermediate third that was not included in the analysis. The average intensity of each pixel row is represented as a dot in the plots. The average row intensity of the polar third (blue) of each row was then compared to the average row intensity of each row of the the mural third (red). Significance assessed by two-tailed unpaired t-test. *** for pvalue<0.001 and * for pvalue<0.05.

bioRxiv preprint doi: https://doi.org/10.1101/510362; this version posted January 3, 2019. The copyright holder for this preprint (which was not certified by peer review) is the author/funder. All rights reserved. No reuse allowed without permission.

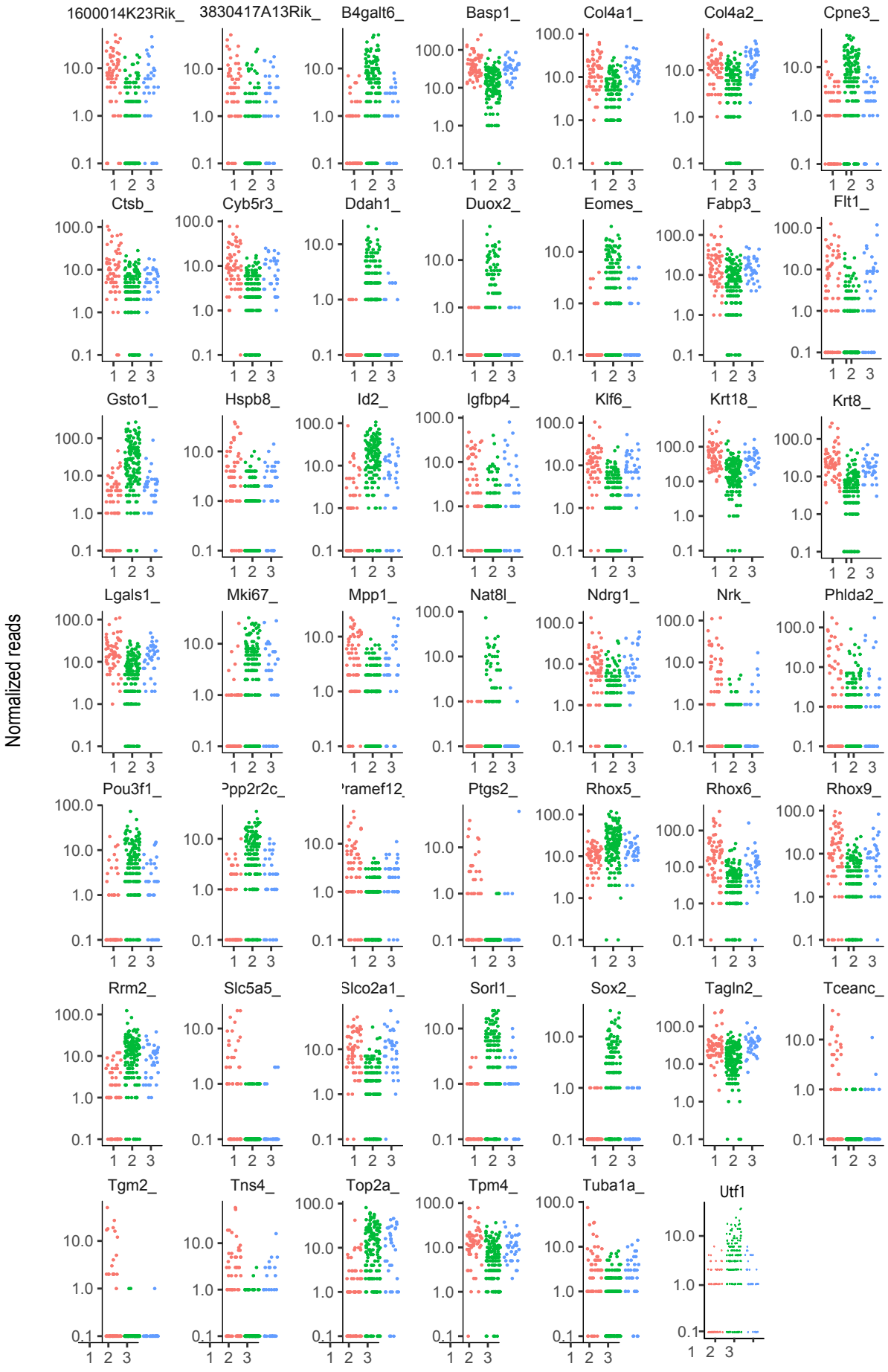

Supplementary figure 5. Jitter plots for the expression of the top 48 differentially expressed genes when comparing clusters 1 and 2.